Physical modeling of seismic illumination and SWD

Joe Wong, Hongliang Zhang, Nasser Kazemi, Kevin Bertram, Kris Innanen, and Roman Shor

ABSTRACT

Surface land and marine seismic data contain reflected waveforms from the subsurface that can be back-propagated through a background medium for imaging purposes. In complex structures, it is possible that wave energy penetrate only weakly into some areas, or not at all causing seismic shadows (i.e., the illumination problem). Deficiencies in seismic illumination can be mitigated if deep subsurface sources are used in acquisition.

Drill-bits generate significant elastic wave at locations deep below the surface. Moreover, since drilling anyway is necessary, using the drill-bit-rock interaction as a seismic source comes with no extra cost or interruption in the drilling process. The possibility exists that the drill-bit is a viable subsurface seismic source and that seismic-while-drilling (SWD) is a practical method for improving seismic illumination.

The CREWES seismic physical modeling group, in collaboration with the University of Calgary Department of Chemical and Petroleum Engineering, has undertaken a physical-modeling project to investigate SWD (seismic-while-drilling). This article reports on the results in regards to both the illumination problem and the recording of complex seismic waveforms.

INTRODUCTION

Surface seismic surveys often encounter geological situations where blocking structures above a target zone create seismic shadows and prevent reflections from deep targets. This seismic illumination problem can be caused by attenuating gas clouds and high-velocity salt zones. In the latter case, complex boundaries between the salt and lower-velocity sedimentary rocks lead to such severe refraction that seismic waves originating from above the salt never reach targets below the salt. Lack of complete illumination from surface-only sources and receivers can be mitigated if boreholes or wells are available to place subsurface sources below the high-velocity salt zones, but access to existing wells for placement of sources is severely restricted because they are used for oil production. However, recording vibrations originating at depth while a well is being drilled would not impact production. The vibrations produced by a drill-bit interacting with rock are complex, but potentially they can be useful for at least partially remedying illumination deficiencies caused by blocking structures.

The drilling process produces vibrations that are non-stationary and of extended duration. Moreover, the source radiation pattern of the drill-bit-rock interaction is unpredictable. If we can account for these issues, SWD would add new measurements and information to seismic migration and imaging, hopefully resulting in clearer images of the subsurface geological structure. Increase in the fidelity of seismic images help guide decisions in both exploration and production, as well as for optimizing drilling parameters (Greenberg, 2008).

We used physical modeling to investigate SWD as a method for mitigating deficiencies in seismic illumination. In the first part of our investigation, we conducted surveys to study a specific illumination problem and its mitigation. We conducted surveys employing impulsive sources to acquire data with surface-only receivers and sources, and then with surface receivers and subsurface sources. In the second part of the investigation, we address the issue of simulating in the modeling laboratory the vibrations produced by drill-bits acting as seismic sources. We need electronically to produce complex non-impulsive high-voltage waveforms that represent the vibrations generated by drilling and use them to drive our subsurface piezoelectric transducer sources. This issue, not solved completely solved at present, is addressed in Appendices A and B.

AN INVESTIGATION OF SEISMIC ILLUMINATION

The simple 2.5 D model shown on Figure 1 was designed to simulate a subsalt imaging problem. We used it to investigate the illumination issues. The upper sill-and-dike structure represents a salt body and is made of acrylic plastic (Plexiglas). Its velocity (2745 m/s) is almost twice as fast as that of the surrounding water. The deeper trapezoidal and hemispheric bodies represent the targets. The upper high-velocity body should act as a blocking structure causing severe refraction of acoustic waves so that, by using surface-only sources and receivers, certain portions of the underlying hemispheric and trapezoid targets will not be illuminated.

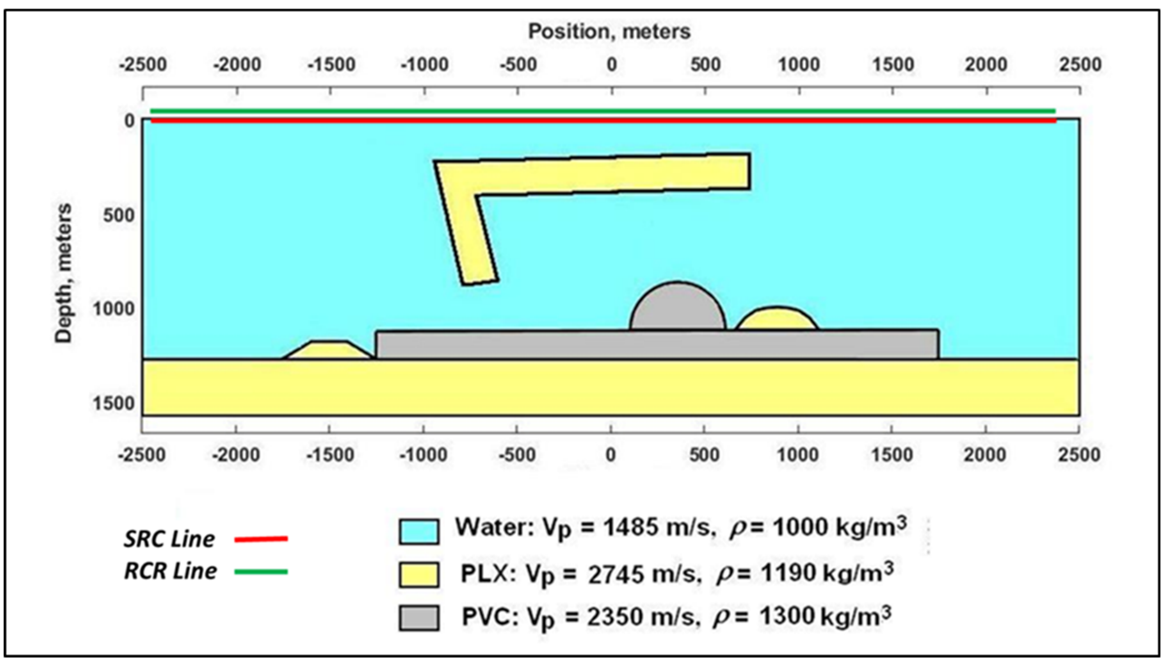

Figure 1: A physical model for studying seismic illumination, showing surface-only sources and receivers. The high-velocity sill-and-dike body acts as a blocking structure. The x-coordinate of all sources and receivers are nominally 0m, and all survey lines run along the y-axis. The water–air interface is about 1350m above the source and receiver survey lines.

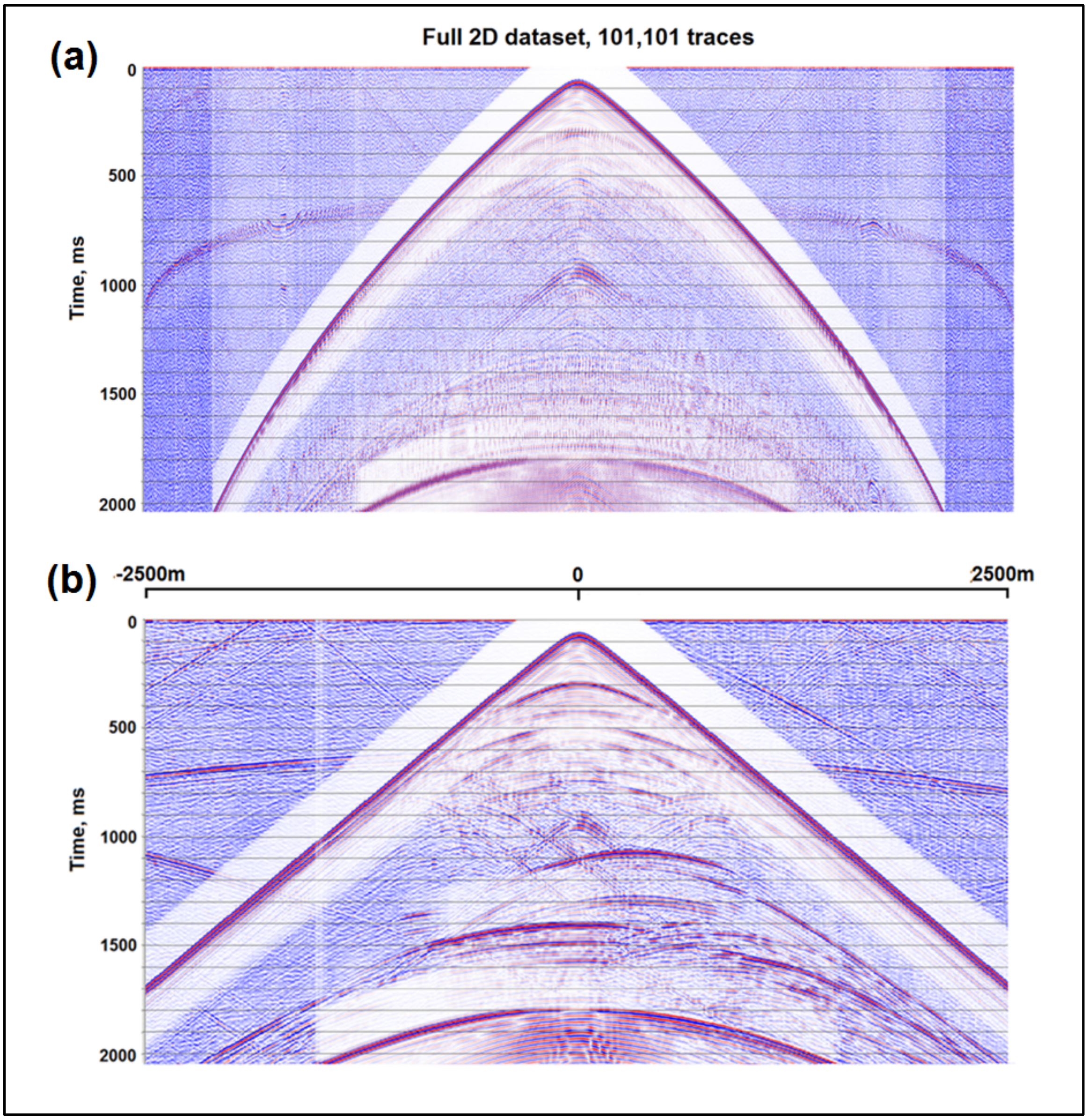

Figure 2: (a) AGC plot of all seismograms from the 2D survey, sorted into common-offset gathers (AGC window=1000ms). The relevant reflections from the targets lie above 1700ms. The hyperbola at 1800-2000ms is the primary reflection from the water-air interface. (b) AGC plot of a sample common-source gather (AGC window=200ms). The bottommost hyperbola is the primary reflection from the water-air interface

We acquired impulsive source data using sources and receivers above the high-velocity blocking structure. A standard 2D survey with 50m source spacing and 5m receiver spacing resulted in 101,101 seismic traces. They are displayed with AGC on Figure 2(a) after sorting into common offset gathers. The seismograms also can be sorted into common-source gathers, an example of which is shown on Figure 2(b). On this figure, reflections from the targets lie above 1700ms. The prominent isolated feature in the middle of the plot at about 900-1000ms is due to an internal multiple reflection in the water column. It is actually quite weak, and appears strong only because of AGC. The hyperbola at 1800-2000ms is the primary reflection from the water–air interface about 1350 above the source and receiver survey lines.

In addition to the normal 2D survey, we also conducted a high-resolution zero-offset survey over the model. The unprocessed data are plotted on Figure 3(a). The display shows reflections from most of the main boundaries, but there also are features that appear to be unrelated to the targets on the schematic diagram of Figure 1. The flat event running right across the display at about 900-950ms is a water-column multiple. Other events are internal multiples, PSP conversions, edge and corner diffractions, out-of-plane diffractions, and reflections from the walls of the water tank holding the model. These extraneous events are quite weak, but appear prominently because of AGC before plotting. The extraneous events likely would pose challenges to imaging algorithms such as two-dimensional RTM or FWI. For the data of Figure 3(a), a simple amplitude discrimination process can remove most of these, as is shown on Figure 3(b). Amplitude discrimination was done in the following way:

1. For every trace, mute the first and last 250ms, and then normalize by the maximum peak-to-peak value.

2. Plot the normalized traces with AGC, save the AGC gains for each trace, and then express the gains in decibe1s.

3. Zero any trace value on the display with AGC gain less than a cut-off level. For trace values above 500ms, the cut-off level was set at –35dB; for trace values below 500ms, the cut-off level was set at -40dB.

4. The amplitude-discriminated AGC traces can be restored to normal amplitude levels by dividing by the saved AGC gains.

Henley and Wong (this volume) discuss more traditional processes (e.g., median filtering and radial trace filtering) to improve the 2D survey data prior to imaging.

In addition to the surface-only surveys, we recorded data with sources at many locations beneath the sill-and-dike shooting up to the surface receiver line (see Figure 4). The subsurface source lines on the figure represent possible positions of a drill-bit acting as a subsurface source. The 41,041 seismograms acquired in such subsurface-to-surface shooting add extra illumination, and help to image that part of the geology not illuminated by surface-only sources and receivers. Figure 5 is a plot of seismograms collected for one such subsurface source. The asymmetrical appearance of this display is caused by the dike portion of the high-velocity blocking structure.

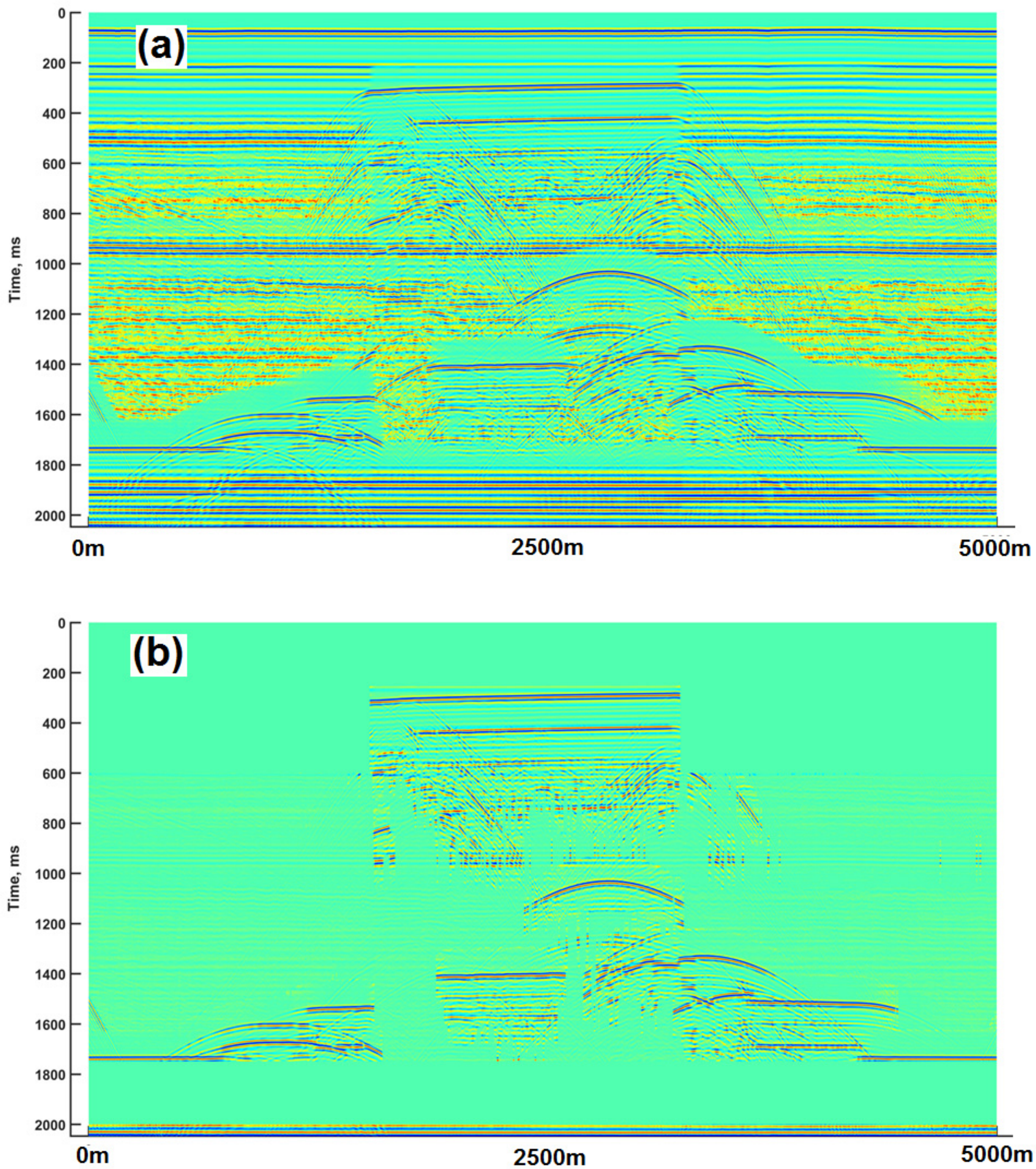

Figure 3: (a) AGC plot of unprocessed data from the high-resolution zer0-offset survey, showing many (low-amplitude) extraneous events that may pose challenges to processing and imaging. Trace spacing is 5m. (b) The same display after applying amplitude discrimination. Reflections from the main boundaries of the physical appear with less interference from extraneous events.

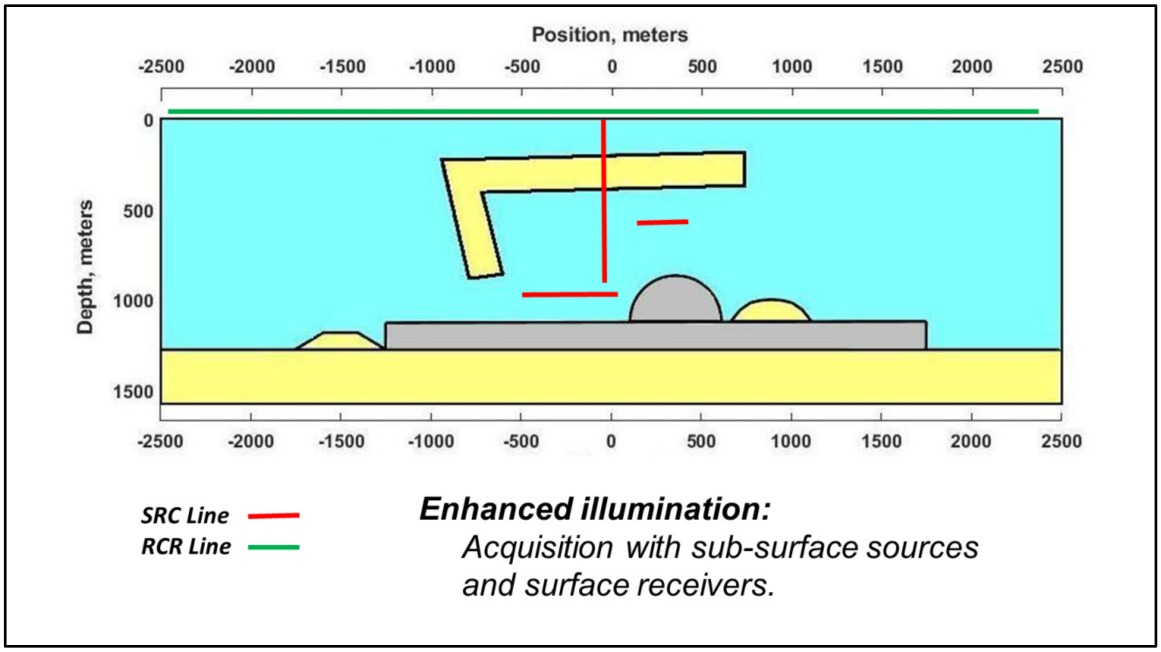

Figure 4: Schematic diagram showing subsurface sources shooting up to a surface receiver line. The subsurface source locations represent positions of a drill-bit acting as a seismic source.

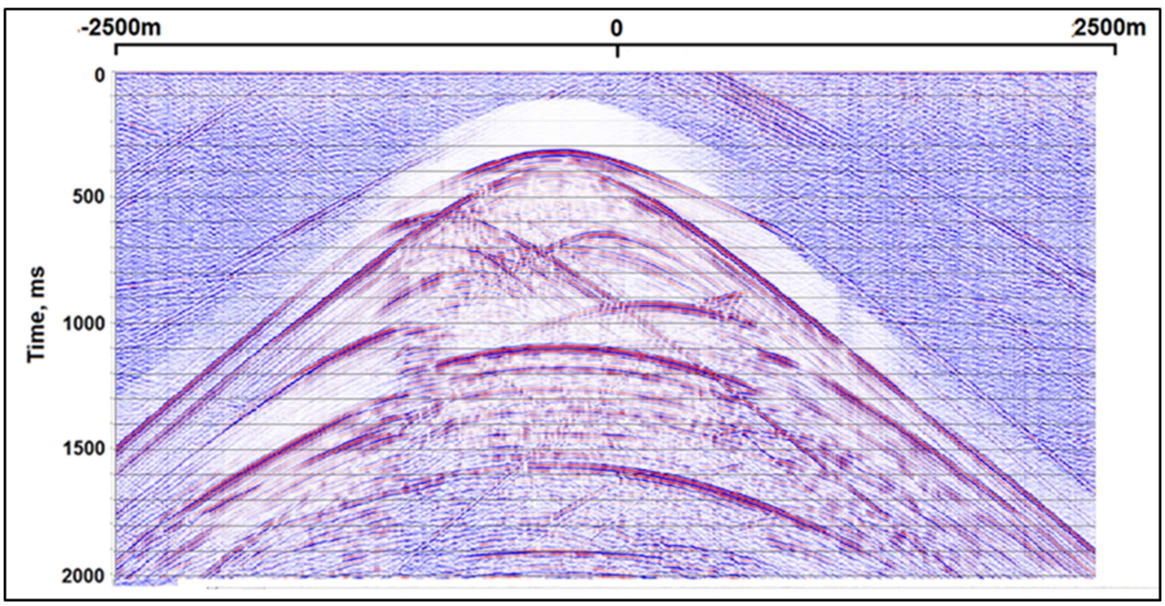

Figure 5: AGC plot of a common-source gather (AGC window=200ms) due to a subsurface source with coordinates (xs,ys,zs) of (0m, 240m, 350m)..Trace spacing is 5m.

The data acquired in this project ultimately will be used to produce a high-fidelity picture of the physical model, i.e., an accurate and reliable image of the acrylic sill-dike structure and the trapezoidal and hemispheric targets below. However, prior to that, we must resolve imaging challenges posed by the following factors:

- radiation/reception patterns of the piezopin transducers,
- non-stationary waveforms,
- PSP conversions,
- internal multiples,
- systematic noise.

The systematic noise arises from water-column multiples, out-of-plane diffractions, reflections from the walls of the water tank, and internal reflections within the geological bodies.

Using the surface-only data, one of us (Kazemi) produced depth-migrated images with a Fourier finite difference migration method (Ristow and Rühl, 1994.). The image shown on Figure 6(a) was produced without suppressing water-column and internal multiples. Fictitious layers can be seen at the bottom of the image since the migration operator does not handle multiples. Figure 6(b) displays the depth image after suppressing multiples before migration. In both cases, the main features of the model are properly imaged, but some boundaries have been distorted. Illumination problems are obvious in the hanging wall of the blocking structure. The blocking structure also generates a shadow zone so that the middle hemispheric target is not properly imaged. We have not yet produced any images that include the data acquired with subsurface sources.

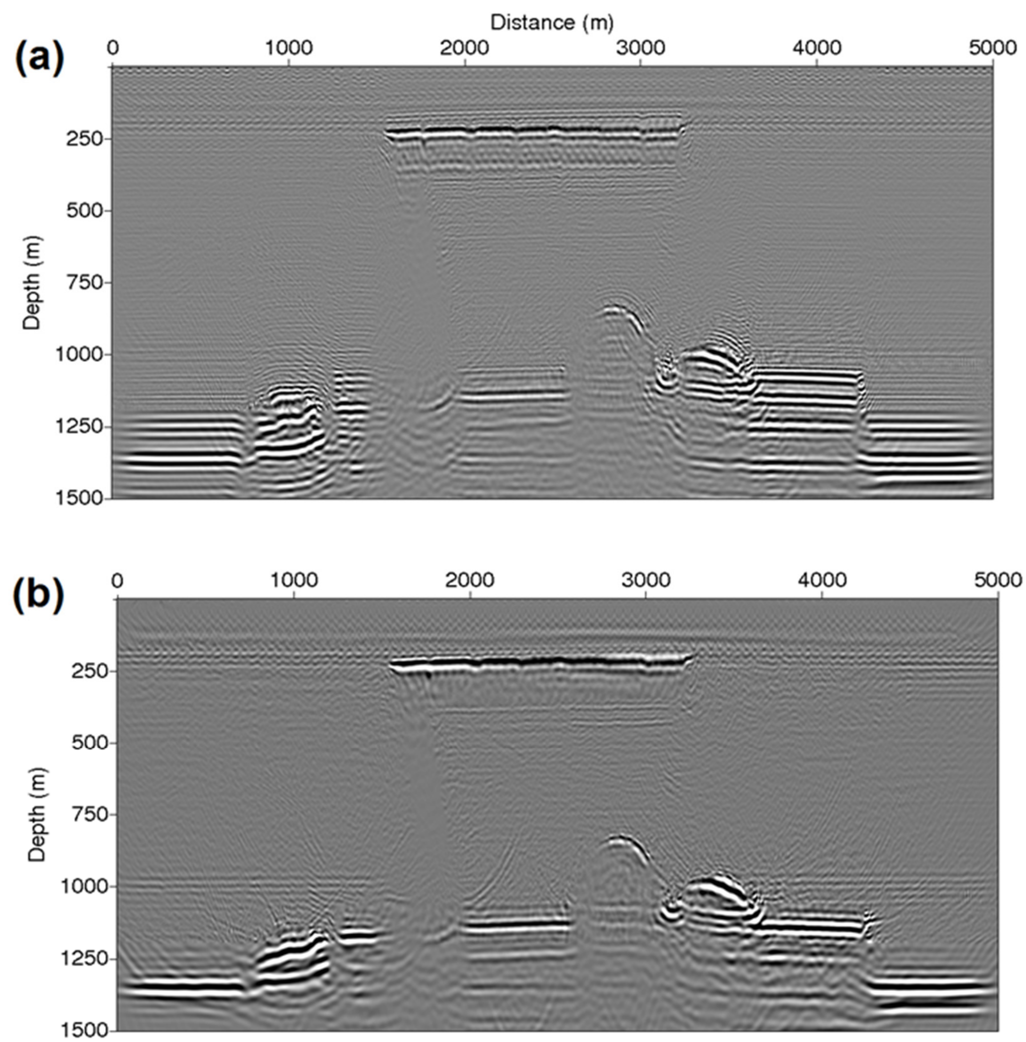

Figure 6: (a) Depth-migrated images produced with surface-only data before multiple suppression. Fictitious layers are present at the base of the model. They can be eliminated by muting amplitudes below 1800ms in all seismograms. (b) Depth-migrated image after suppression of multiples. In both cases, the dike, the bottom boundary of the sill, and the deeper targets are not well imaged.

SUMMARY AND CONCLUSION

We have designed a physical model consisting of a high-velocity sill-and-dike structure immersed in water overlying deeper trapezoidal and hemispheric targets. Using surface-only sources and receivers, we completed a conventional 2D seismic survey and a high-resolution zero-offset survey over this model. As expected, the overlying high-velocity structure blocked seismic energy from reaching portions of the deeper target. These deficiencies in seismic illumination degrade depth images produced by a Fourier finite-difference migration routine. To enhance the illumination of the deeper targets, we also recorded data with sources below the blocking structure shooting up to surface receivers. We expect that depth imaging with information added from the subsurface-to-surface shooting will help better define the deep targets as well as the overall geological structure of the model. At present, such imaging remains to be done.

A drill-bit interacting with solid rock at depth is a convenient and inexpensive subsurface seismic source. The interaction produces strong vibrations with complex wave shapes of long duration. These are much different from the waveforms produced by conventional impulsive sources. The physically-modeled seismic data acquired with subsurface-to-surface shooting sources were all recorded with impulsive sources because we have not yet been able reliably to drive a piezoelectric transducer with arbitrary waveforms. However, the impulsive seismograms already acquired can be convolved numerically with any SWD source waveform to produce traces that appear like the vibrations recorded from a drill-bit (see Appendix B).

On this last point, we are working on using a Raspberry Pi microcomputer to generate arbitrary and complex source functions with 0.1 microsecond precision. At present, we can produce signals with the required amplitudes and polarities, but we have not achieved the required timing precision. The source of the problem is that the operating system of the microcomputer generates interrupt calls that disrupts the output timing of data for external use. We have found a method for disabling the interrupt calls; we will test this method in the near future. Once the system interrupts are disabled, we will obtain the required timing precision. More discussion on this problem is found in Appendix A.

ACKNOWLEDGEMENTS

We thank the sponsors of CREWES for continued support. This work was funded by CREWES industrial sponsors, NSERC (Natural Science and Engineering Research Council of Canada) through the grant CRDPJ 461179-13, and in part by the Canada First Research Excellence Fund.

REFERENCES

Henley, D. A., and Wong, J., Let there be light: illuminating physical models from the surface: CREWES Research Report, this volume.

Kazemi, N., and Sacchi, M. D., 2014, Sparse multichannel blind deconvolution: Geophysics, **79**, No. 5, V143–V152.

Kazemi, N., Shor, R., and Innanen, K., 2018a, Illumination compensation with seismic-while-drilling plus surface seismic imaging, in 80th EAGE Conference and Exhibition 2018.

Kazemi, N., Trad, D., Innanen, K., and Shor, R., 2018b. Least-squares RTM of a seismic-while-drilling dataset: CREWES Research Reports, **30**, 1-10.

Greenberg, J., 2008, Seismic while drilling keeps bit turning to right while acquiring key real-time data: Drilling Contractor, **64**, No. 2, 44–45.

Poletto, F., 2005, Energy balance of a drill-bit seismic source, part 1: Rotary energy and radiation properties: Geophysics, **70**, No. 2, T13–T28.

Ristow, D., Rühl, T., 1994, Fourier finite-difference migration: Geophysics, **59**, No. 12, 1882-1893.

Wong, J., Zhang, H., Bertram, K., and Innanen, K., Microseismic and time reversal physical modeling: CREWES Research Report, this volume.

APPENDIX A: GENERATING COMPLEX SOURCE WAVEFORMS

A major difference between the conventional surface seismic data and the SWD data is in the source signature. In the case of SWD acquisition, the drill bit-rock interaction generates correlative and non-impulsive vibrations that act as the source signature. To numerically model these vibrations produced at the point of drilling, we assume that every tooth of the drill bit generates a harmonic waveform (Poletto, 2005). Depending on the hardness, brittleness, and velocity of rocks and the drilling parameters, the drill-bit source signature will have varying harmonic and non-harmonic components due to the resonances between the drill string and rocks at the source location. Figure A1 shows one result of numerically modeling the drill-bit source signature (band-limited white Gaussian noise also may be added).

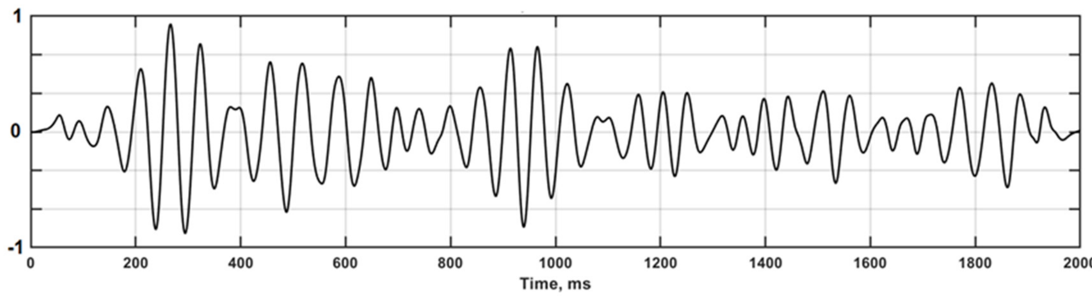

Figure A1: A possible source signature produced by a drill-bit interacting with rock.

To fully simulate SWD acquisition in physical modeling, we must electronically generate a high-voltage version of Figure A1 to drive our piezoelectric source transducers. Current research in the Seismic Physical Modeling Laboratory is aimed at achieving this goal.

Figure A2 is a schematic showing a prototype electronic circuit capable of producing long-duration high-voltage signals suitable for driving piezopin source transducers. A defined arbitrary waveform is produced by a C or MATLAB program and saved in a file on a Raspberry Pi (3B+ or 4) microcomputer running a version of the LINUX operating system. A compiled C program reads the file and stores the waveform in memory. The program converts the waveform into 8-bit or 10-bit integer words and outputs the bits to a digital-to-analogue converter (a DAC, either a dedicated integrated circuit or an R2R ladder) via the GPIO (general purpose input-output) pins of the Raspberry Pi. The output must be sent at precise rates on the order of one word every 500 nanoseconds. The DAC output is filtered and amplified to yield peak-to-peak voltage of about 200-300 volts. The high-voltage signal (with bandwidth approximately from 100 kHz to 1.0 MHz) is used to drive the piezoelectric source transducer.

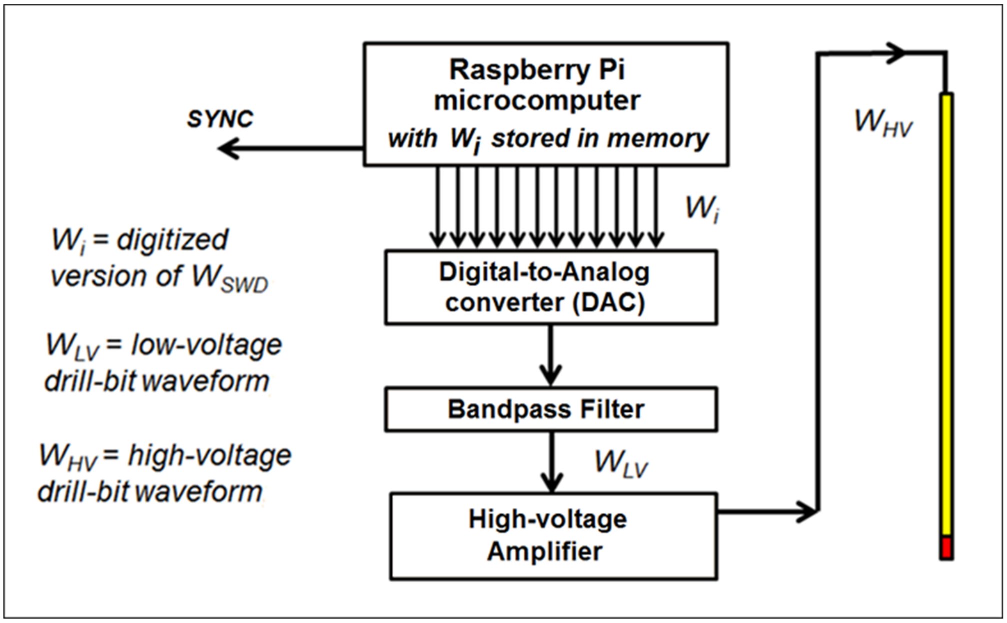

Figure A2: Schematic diagram showing an electronic design for producing high-voltage waveforms for driving a piezopin source transducer (shown in yellow). The SYNC signal is needed for synchronized stacking of received seismograms.

The Raspberry Pi is a small microcomputer with a credit-card size footprint. In the Model 3B+ version it has a system clock that runs at 14 GHz, so sending 10-bit signals out at 10MHz speeds via its GPIO pins is no problem. However, in working with prototypes based on Figure A2 we have discovered a major obstacle. The LINUX operating system running the microcomputer generates system interrupt calls that disrupt the precise timing of the output signals. Such interrupt calls must be disabled. We also need a high-frequency, high-voltage amplifier the raises the low-level (3.5 volts) output signals from the Raspberry PI to levels needed to drive our piezoelectric sources (200 to 300 volts).

Neither of these issues is insurmountable. There already exists an open-source C program for the Raspberry PI that disables and enables system interrupts. We have a concept for building a high-speed, high-voltage amplifier using power MOSFETs. In the coming year we will actively pursue these and other possible solutions.

By adding the capability of driving source piezoelectric transduces with complex waveforms, we increase the flexibility of the University of Calgary Seismic Physical Modeling Facility to conduct several different and interesting experiments. For example, in the time-reversal described by Wong et al. (this volume), we need to drive sources in real time with waveforms that are mirrored, windowed, and time reversed versions of received seismograms.

APPENDIX B: DECONVOLVING SWD SEISMOGRAMS

The vibrations produced by a rotating drill-bit cutting rock are highly complex, non-impulsive, and non-stationary (see Figure B1). As a result, data recorded with a SWD source do not resemble seismic data produced by conventional impulsive sources. Although Kazemi et al. (2018a, b) have proposed using SWD vibration traces directly in a least-squares RTM depth imaging algorithm, it may be essential that they be deconvolved to recover impulsive seismograms suitable for visual examination or for other imaging schemes.

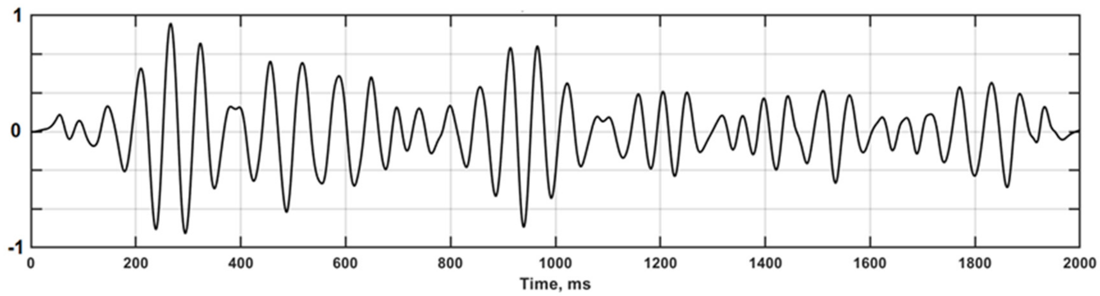

Figure B1: A possible source signature produced by a drill-bit interacting with rock.

Figures B2 and B3 indicate why deconvolution might be necessary. Figure B2 shows a common-source gather recorded with a subsurface source activated with an impulse. While we are not able yet to drive the source with the drill-bit waveform on Figure B1, we can use it to convolve numerically every trace on Figure B2 to produce the Figure B3 display of what SWD data might look like if we were able to do so. The result of the convolution is plotted on Figure B3.

On the display of impu1sive seismograms on Figure B2, we are able to discern individual seismic arrivals and evaluate the quality of the entire gather. It is impossible to do this by looking at the display of the SWD traces on Figure B3. Deconvolution of the SWD data would be highly desirable, if only for this reason.

One deconvolution method is shown on Figures B4 and B5, where the convolution of an impulsive signal with the drill-bit waveform is undone in frequency domain. Convolution in time domain is equivalent to multiplication in frequency domain, and deconvolution in time domain is equivalent to division in frequency domain. However, this method is very sensitive to noise. Likely a more stable alternative to finding the impulsive signal will be required for field data, e.g., least-squares fitting and linear optimization, or sparse blind deconvolution (Kazemi and Sacchi, 2014).

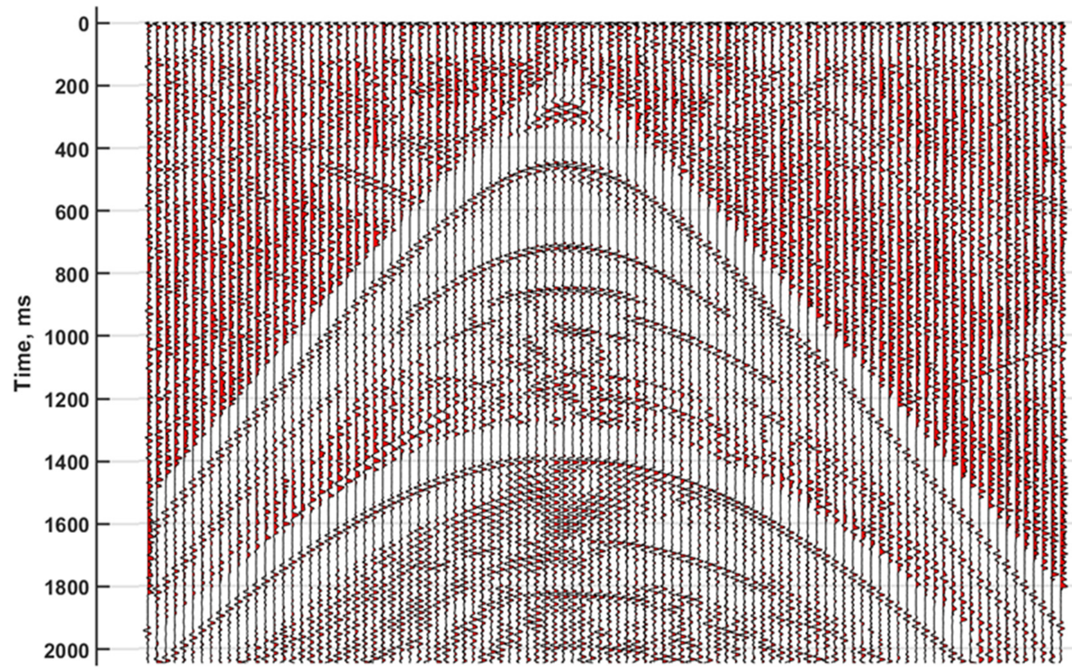

Figure B2: AGC display of a common-source gather recorded with an impulsive subsurface source (AGC window = 200ms). Individual seismic arrivals are clearly discernible.

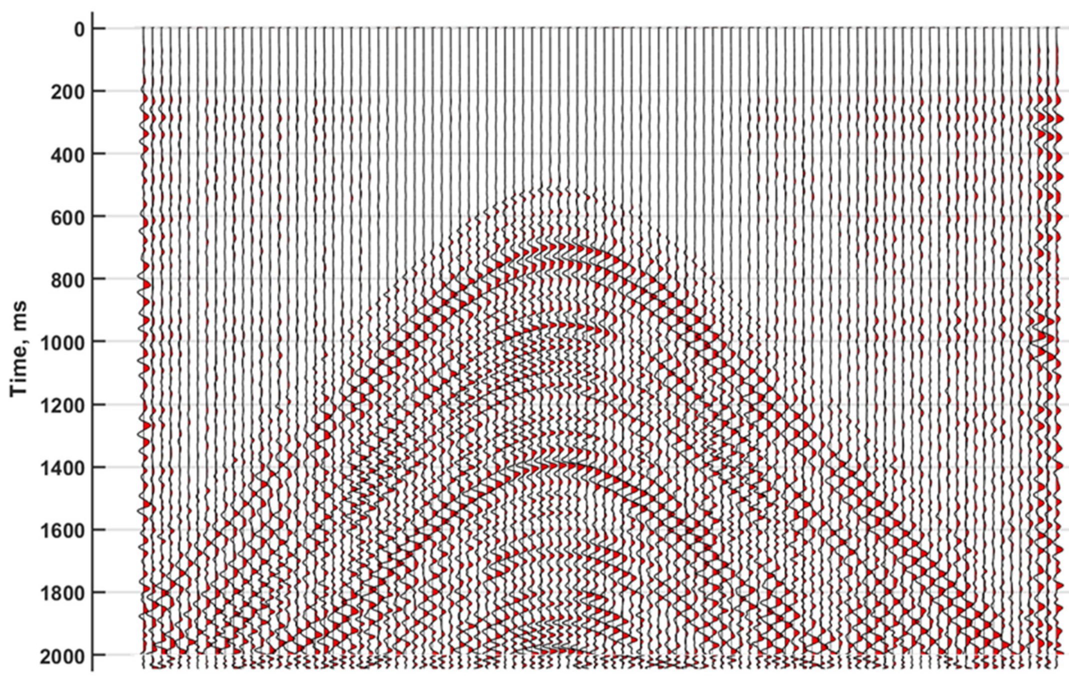

Figure B3: Normalized display of the common-source gather in Figure B2 convolved with the drill-bit signal on Figure B1. It is not possible to see individual seismic arrivals clearly.

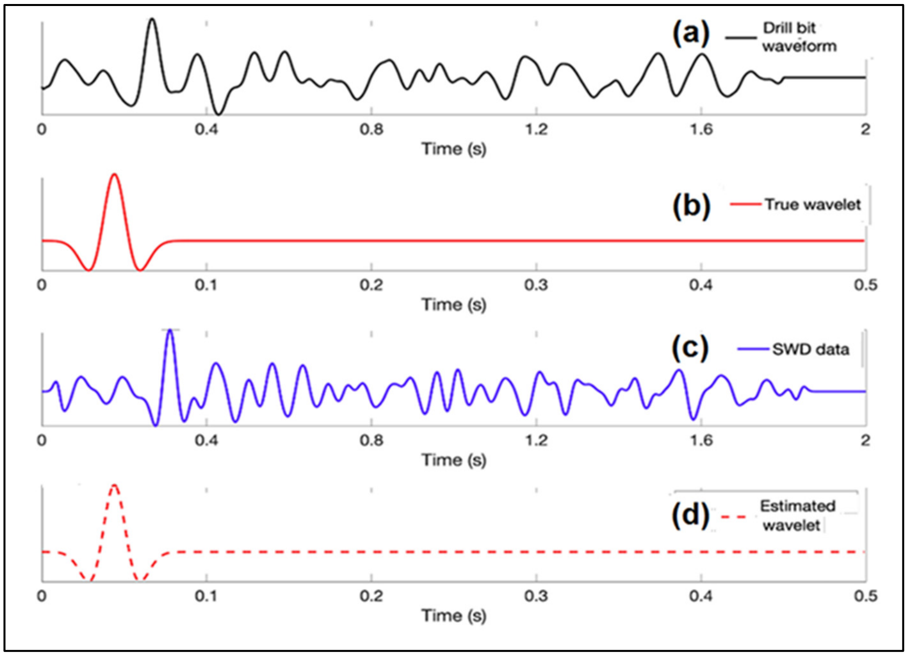

Figure B4: Time-domain convolution and deconvolution of a drill-bit waveform (a) with an impulse-response wavelet (b). In SWD acquisition, recorded trace (c) is the convolution of ((b) with (a). Trace (d), a version of trace (b) estimated from trace (c), is recovered by deconvolution.

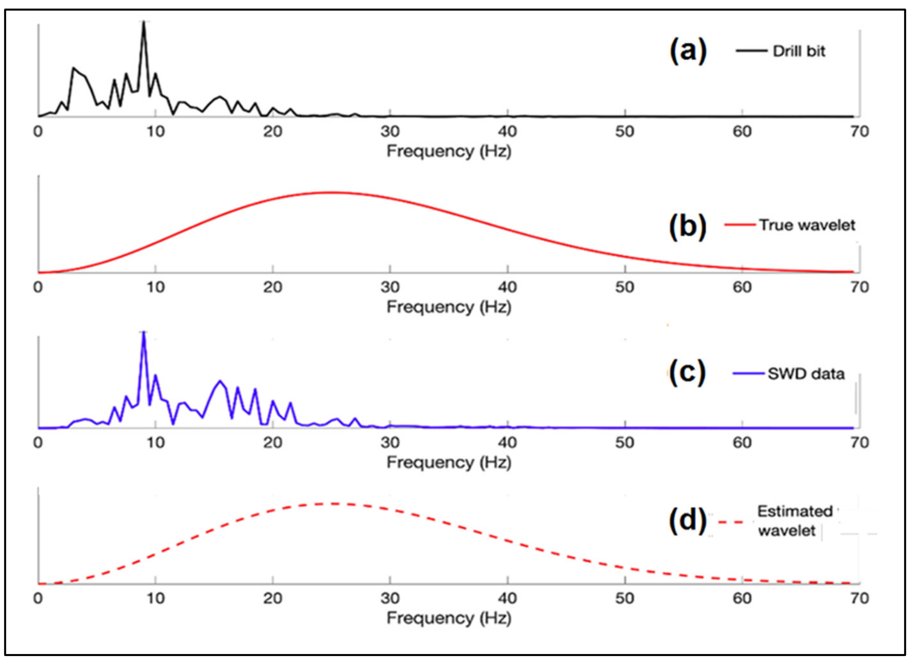

Figure B5: Frequency-domain equivalent of convolution and deconvolution of a drill-bit waveform with an impulse-response wavelet: Spectrum (c) is the product of spectra (a) and (b); Spectrum (d) is spectrum (c) divided by spectrum (a) plus a small stabilizing factor.